Excess cholesterol induces mouse egg activation and may cause female infertility

Ayce Yesilaltay[a,1], Gregoriy A. Dokshin[a,b,1], Dolores Busso[c,1], Li Wang[a,1], Dalia Galiani[d], Tony Chavarria[e], Eliza Vasile[f], Linda Quilaqueo[c], Juan Andrés Orellana[g], Dalia Walzer[a], Ruth Shalgi[h], Nava Dekel[d], David F. Albertini[i], Attilio Rigotti[c], David C. Page[a,b], and Monty Krieger[a,2]

Departments of [a]Biology and [e]Comparative Medicine and [f]The Koch Institute, Massachusetts Institute of Technology, Cambridge, MA 02139; [b]Howard Hughes Medical Institute, Whitehead Institute, Cambridge, MA 02142; [c]Departamento de Nutrición, Diabetes y Metabolismo and [g]Departamento de Neurología, Pontificia Universidad Católica de Chile, 8330024 Santiago, Chile; [d]Department of Biological Regulation, The Weizmann Institute of Science, Rehovot 76100, Israel; [h]Department of Cell and Developmental Biology, Sackler Faculty of Medicine, Tel Aviv University, Tel Aviv 69978, Israel; and [i]Department of Molecular and Integrative Physiology, Institute for Reproductive Health and Regenerative Medicine, University of Kansas Medical Center, Kansas City, KS 66160

Contributed by Monty Krieger, October 7, 2014 (sent for review July 22, 2013)

The HDL receptor scavenger receptor, class B type I (SR-BI) controls the structure and fate of plasma HDL. Female SR-BI KO mice are infertile, apparently because of their abnormal cholesterol-enriched HDL particles. We examined the growth and meiotic progression of SR-BI KO oocytes and found that they underwent normal germinal vesicle breakdown; however, SR-BI KO eggs, which had accumulated excess cholesterol in vivo, spontaneously activated, and they escaped metaphase II (MII) arrest and progressed to pronuclear, MIII, and anaphase/telophase III stages. Eggs from fertile WT mice were activated when loaded in vitro with excess cholesterol by a cholesterol/methyl-β-cyclodextrin complex, phenocopying SR-BI KO oocytes. In vitro cholesterol loading of eggs induced reduction in maturation promoting factor and MAPK activities, elevation of intracellular calcium, extrusion of a second polar body, and progression to meiotic stages beyond MII. These results suggest that the infertility of SR-BI KO females is caused, at least in part, by excess cholesterol in eggs inducing premature activation and that cholesterol can activate WT mouse eggs to escape from MII arrest. Analysis of SR-BI KO female infertility raises the possibility that abnormalities in cholesterol metabolism might underlie some cases of human female infertility of unknown etiology.

fertility | egg | cholesterol | HDL | meiosis

Scavenger receptor, class B type I (SR-BI) is an HDL receptor that transports unesterified cholesterol (UC) and its esters between lipoproteins and cells (1–3) and functions as a signaling receptor (4). SR-BI controls the structure and composition of plasma HDL and the amounts and fates of HDL cholesterol (2, 3, 5, 6). Homozygous null SR-BI knockout (KO) mice exhibit hypercholesterolemia with unusually large and UC-enriched HDL particles [abnormally high UC to total cholesterol (TC) ratio] (5, 7, 8). This unusual hypercholesterolemia apparently induces a deleterious accumulation of UC in RBCs and platelets that influences their maturation, lifetime in the bloodstream, structure, and/or function (7–13).

Female but not male SR-BI KO mice exhibit fully penetrant infertility, despite their essentially normal ovarian histology (6, 14). Several lines of surgical transplantation, genetic, histologic, and pharmacologic evidence indicate that the abnormal structure and composition of circulating HDL in SR-BI KO mice contribute to their female infertility (*Discussion*). This infertility can be effectively corrected by altering (through a variety of approaches) the structure and abundance of the circulating HDL to which the ovaries are exposed (7, 14, 15). This evidence also suggests that the infertility is likely caused by defects in oocytes/eggs manifested during the periovulatory period without affecting the primordial follicle pool. Indeed, ∼19% of the ovulated eggs harvested ∼16 h after hormone-induced superovulation are dead (6, 14) (see below). The remaining oocytes are unable to be fertilized or develop into viable pups. Here, we examined SR-BI KO oocyte growth and progression through the peri- and post-ovulatory stages of meiosis (Fig. 1) and investigated the possibility that high levels of UC in HDL might result in excess cholesterol deposition in oocytes or eggs that might influence their growth, meiotic progression, and/or viability.

Normally, after the luteinizing hormone surge of the estrous cycle and just before ovulation, mammalian oocytes complete the first meiotic division [meiosis I (MI)] and immediately thereafter proceed to metaphase II (MII), a stage at which they arrest (Fig. 1). A complex network of proteins and intracellular signals establishes and maintains MII arrest [e.g., elevated MAPK and maturation promoting factor (MPF; or cdk1/cyclin B) kinase activities] (16, 17) and subsequently permits exit from this stage after fertilization (e.g., reduction in MAPK and MPF activities) (16, 17). Productive fertilization of MII-arrested eggs leads to inositol triphosphate-induced oscillations in intracellular calcium concentration ($[Ca^{2+}]_i$) that activate the eggs [exit from MII arrest, second polar body (PB) extrusion, formation of pronuclei, etc.] (Fig. 1) (18, 19). Fertilization-induced changes in intracellular zinc levels also may influence activation (19). The parthenogenetic stimulant $SrCl_2$ activates normal eggs (20) by inducing oscillations in $[Ca^{2+}]_i$ (21, 22) and suppressing MAPK and MPF kinase activities (23) that mimic those that occur after fertilization (21, 22). Brief exposure to ethanol induces a single spike in $[Ca^{2+}]_i$ and activates eggs (24, 25). Unlike fertilized eggs,

Significance

Production of functional sperm and eggs requires a complex process called meiosis. Meiosis in mouse and human eggs pauses at a stage called metaphase II (MII) arrest until fertilization by sperm. After fertilization, eggs released from MII arrest complete meiosis and develop into new individuals. In analyzing the female infertility of genetically altered mice, we discovered that excess cholesterol can trick mouse eggs into behaving as though they were fertilized (released from arrest), thus disrupting the normal synchrony between fertilization and completion of meiosis and rendering them dysfunctional. These findings suggest that abnormal cholesterol metabolism may contribute to some forms of human female infertility.

Author contributions: A.Y., G.A.D., D.B., L.W., D.G., E.V., R.S., N.D., D.F.A., A.R., D.C.P., and M.K. designed research; A.Y., G.A.D., D.B., L.W., T.C., E.V., L.Q., and D.W. performed research; J.A.O. contributed new reagents/analytic tools; A.Y., G.A.D., D.B., L.W., E.V., D.C.P., and M.K. analyzed data; and A.Y., G.A.D., D.B., L.W., R.S., N.D., and M.K. wrote the paper.

The authors declare no conflict of interest.

[1]A.Y., G.A.D., D.B., and L.W. contributed equally to this work.

[2]To whom correspondence should be addressed. Email: krieger@mit.edu.

This article contains supporting information online at www.pnas.org/lookup/suppl/doi:10.1073/pnas.1418954111/-/DCSupplemental.

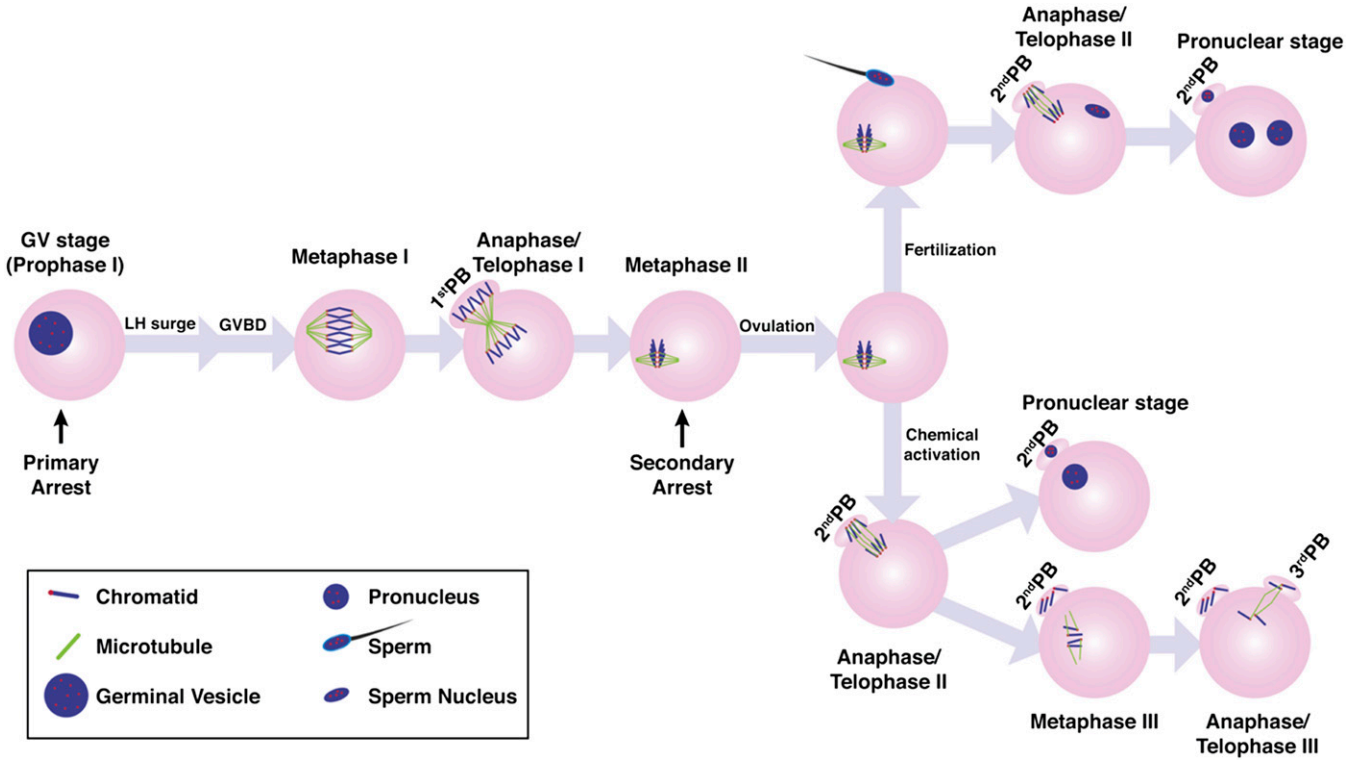

Fig. 1. Meiotic resumption and egg activation in the mouse. Schematic representation of meiotic resumption and egg activation by either fertilization or chemical agents. The stages at which primary (prophase I) and secondary (MII) arrest occur are indicated. Oocytes initiate meiosis during fetal development and enter primary arrest at the diplotene stage of prophase I around the time of birth (not illustrated here). Prophase I arrest is maintained during oocyte growth and differentiation. Prior to ovulation, meiosis resumes, the nuclear envelope of the germinal vesicle (GV) dissassembles [GV breakdown (GVBD)], and chromosomes condense and align on the first metaphase plate. During the first division, homologous chromosomes segregate and the first polar body (PB) is extruded (first PB in anaphase/telophase I). The remaining chromosomes realign on the second metaphase plate (MII) followed by secondary arrest. During MII arrest, the first PB often degrades. Eggs that are ovulated can exit MII arrest and complete meiosis when activated by a fertilizing sperm (upper right) or chemical agents, such as $SrCl_2$ or ethanol (lower right), which induce a spike (ethanol) or oscillations (sperm and $SrCl_2$) in cytoplasmic Ca^{2+} levels and suppress MAPK and MPF activities. On activation, sister chromatids segregate, and the second PB is extruded (second PB in anaphase/telophase II). The activated egg then progresses to pronuclear stage as the nuclear envelope reforms. On chemical activation, the egg can alternatively progress to metaphase III, segregate the remaining chromatids randomly during anaphase III, and extrude a third PB (anaphase/telophase III).

which receive the paternal chromosome complement from the sperm, $SrCl_2$- or ethanol-activated eggs are haploid (Fig. 1) and cannot support proper embryogenesis (22).

Here, we found that, within follicles of hormone-treated SR-BI KO females, oocytes apparently resumed meiosis normally. However, these cells spontaneously escaped MII arrest, exhibited reduced MPF and MAPK activities, and aberrantly progressed to haploid pronuclear, metaphase III, and anaphase/telophase III stages, similar to normal ovulated eggs after chemical (e.g., $SrCl_2$) (22, 25) activation (Fig. 1). Compared with control eggs, the eggs of SR-BI KO females accumulated excess cholesterol. Strikingly, we could recapitulate the apparently spontaneous activation of ovulated SR-BI KO eggs in eggs ovulated from fertile control mice (WT or *SR-BI*$^{+/-}$) by treating those eggs with a cholesterol/methyl-β-cyclodextrin (MβCD) complex to load them with excess cholesterol (26). In addition, cholesterol loading induced a single spike in $[Ca^{2+}]_i$ reminiscent of that seen in ethanol-activated eggs (24, 25). These results establish that excess cholesterol loading provides a new approach to activating mammalian MII-arrested eggs and suggest that the infertility of SR-BI KO females is caused, at least in part, by excess cholesterol acting directly on the egg to induce premature activation. Analysis of SR-BI KO female infertility also raises the possibility that abnormalities in cholesterol metabolism might underlie some forms of human female infertility of unknown etiology.

Results

Our previous studies involving restoration of fertility by ovary transplantation and drug treatment suggested that the infertility of SR-BI KO (*SR-BI*$^{-/-}$) female mice is unlikely to be caused by irreversibly impaired early oogenesis or abnormal folliculogenesis (2, 6, 7, 14) (*Discussion*). Rather, the infertility seems likely to be related to defects in oocyte growth, maturation, or activation. SR-BI KO females ovulate almost normal numbers of eggs (6). However, on their recovery from the oviduct, a substantial fraction of the ovulated eggs displays an abnormal, nonrefractile morphology characteristic of dead eggs (the criterion used to score for death here). On average, 4% of ovulated eggs from control *SR-BI*$^{+/-}$ females (n = 47 animals) and 19% of eggs from SR-BI KO females (n = 39 animals) were dead when harvested at 13–16 h after induction of superovulation with human chorionic gonadotropin (hCG) (*Materials and Methods*). The death rate of eggs from SR-BI KO females increased to 53% (n = 7) when they were collected 18–19 h post-hCG injection. Moreover, the viable ovulated eggs cannot be successfully fertilized in vivo to form either early embryos or viable pups. In an effort to better understand the infertility of SR-BI KO females, we investigated events in oocyte development after the *SR-BI*$^{-/-}$ oocytes are recruited from the primordial follicle pool. For many of the experiments reported here, we compared results obtained from SR-BI KO oocytes with those from control *SR-BI*$^{+/-}$ and WT *SR-BI*$^{+/+}$ oocytes or eggs, all of which are from mice on

a 50:50 C57BL/6:129 genetic background (*Materials and Methods*). In some experiments, we used eggs from females on a WT, pure C57BL/6 background.

Oocyte Follicular Growth. Oocytes of the primordial follicle pool arrested in prophase I of meiosis (Fig. 1) are recruited to grow and differentiate throughout the mouse's reproductive lifetime. As oocytes grow, their volume increases proportionally to the volume of the encasing follicle. In rodents, the relative oocyte to follicle diameter from intact follicles of unprimed females has been used as an indicator of follicular oocyte growth (27, 28). We mechanically isolated murine follicles from both SR-BI KO mice and fertile *SR-BI*$^{+/-}$ controls at different stages of development from unprimed sexually immature (prepubertal) 3-wk-old and mature 6-wk-old females. The oocyte and follicle diameters were measured as described in *Materials and Methods*. Fig. 2 *A* and *B* shows that, at both ages, there were linear relationships between the oocyte and follicle diameters and that the slopes of these lines were virtually identical for the follicles and oocytes from SR-BI KO females and *SR-BI*$^{+/-}$ controls. Thus, SR-BI deficiency does not seem to alter the growth of oocytes and their surrounding follicles.

Meiotic Resumption and Extrusion of the First PB. An important indicator of oocyte quality is the ability to resume and complete meiosis, a process called maturation (29). In mice, oocytes initiate meiosis during fetal development and progress through prophase I until the diplotene stage, where they enter primary arrest (Fig. 1). These primordial oocytes acquire the competence to resume meiosis during the late stages of growth and differentiation. In full-grown oocytes, primary arrest is maintained by the follicular soma and relieved before ovulation. Oocytes that resume meiosis undergo germinal vesicle breakdown (GVBD), assemble chromosomes on the first metaphase plate, and complete the first meiotic division, which is accompanied by extrusion of the first PB (Fig. 1). Oocytes then assemble the remaining single set of homologous chromosomes on the second metaphase plate and enter secondary arrest (MII arrest) (Fig. 1).

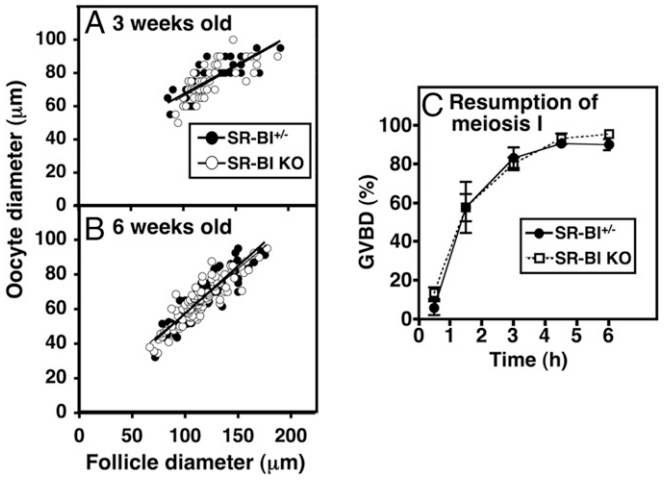

Fig. 2. Oocyte growth and meiotic resumption. (*A* and *B*) Follicles were mechanically isolated from either fertile control *SR-BI*$^{+/-}$ (black circles and thick lines) or infertile SR-BI KO (*SR-BI*$^{-/-}$; white circles and thin lines) mice at (*A*) 3 (unprimed sexually immature) or (*B*) 6 wk of age (mature). The follicles were fixed, and follicle and oocyte diameters were measured as described in *SI Materials and Methods*. The almost superimposed thick and thin lines represent results of linear least squares analysis. The numbers of follicles/oocytes examined at 3 and 6 wk were control *SR-BI*$^{+/-}$ (49 and 89, respectively) and SR-BI KO (50 and 107, respectively). (*C*) GVBD is a spontaneous and dynamic process that begins as early as 30 min after oocytes are placed in culture and reaches its maximum 4–6 h later. Two- to five-mo-old control *SR-BI*$^{+/+}$ (black circles) and SR-BI KO (white squares) females were synchronized by priming with pregnant mare serum gonadotropin; 46 h later, GV oocytes were retrieved by follicular puncture and cultured in M16 media containing the phosphodiesterase inhibitor 3-isobutyl-1-methylxanthine (IBMX) to maintain high levels of cAMP and thus, arrest at the GV stage. The cumulus cells were removed (*SI Materials and Methods*), and the cumulus-free oocytes were transferred to M16 medium without IBMX. At the indicated times thereafter, the percentage of oocytes undergoing GVBD was scored by microscopic examination. The data were pooled from two independent experiments with ≥10 oocytes per female and three females of each genotype per experiment.

Full-grown, prophase I-arrested oocytes in the ovary can be triggered to resume meiosis and progress to MII and secondary arrest by removing them from their follicles. Thus, to investigate whether full-grown oocytes from the SR-BI KO mice and SR-BI$^{+/-}$ controls were competent to resume meiosis, we isolated them from ovaries of unprimed females by follicular puncture and cultured them for 14 h. Resumption and completion of MI were scored by determining by microscopic examination GVBD and first PB extrusion, respectively (*Materials and Methods*). Table S1 shows that the fractions of *SR-BI*$^{+/-}$ and SR-BI KO oocytes undergoing GVBD were similar (87% and 74%, respectively), and the fractions of oocytes extruding the first PB were also similar (78% and 64%, respectively). Fig. 2*C* shows that the rate of GVBD in oocytes from SR-BI KO animals was similar to that for *SR-BI*$^{+/-}$ controls. These results indicate that the rate at and extent to which SR-BI KO oocytes resume (GVBD) and complete MI (first PB extrusion) are similar to those of control, fertile oocytes, indicating that they are competent to resume meiosis.

Spontaneous Progression Beyond MII Arrest. After completion of MI, WT eggs, which still reside in the ovarian follicles, arrest at MII, at which point they are ovulated. The ovulated eggs in the oviduct remain arrested at MII until they are activated by sperm during fertilization, which triggers the completion of meiosis II and the extrusion of the second PB (Fig. 1). Eggs can also activate spontaneously (e.g., during aging) or artificially (e.g., by treatment with chemicals, such as $SrCl_2$/EGTA, ionophores, or ethanol) (30–33). To study postovulatory events in eggs from SR-BI KO mice, we harvested morphologically live eggs from the oviducts of hormone-primed SR-BI KO and control *SR-BI*$^{+/-}$ females either ~16 or ~20 h after hCG administration. We determined the meiotic stage of both control *SR-BI*$^{+/-}$ and SR-BI KO eggs by examining their chromosome/nuclear and spindle organizations. Fig. 3 shows eggs that were stained using a whole-mount preparation technique and imaged by deconvolution microscopy to visualize the DNA (DAPI, blue), microtubules (anti-tubulin, green), nuclear envelope (anti-lamin B1, see Fig. S1), and centromeres (anti-centromere antibody, red). We present the 3D organization of chromosomes in the egg and its PB as a *z* stack of deconvolved images. After image collection and processing, we scored the meiotic state of each egg by determining the number of chromatids by counting centromeres (one chromatid per centromere) in the egg and its PB as well as scoring the morphology of the spindle and the presence or absence of the nuclear lamina. The results are presented in Table 1, and representative images are shown in Fig. 3.

The two leftmost columns in Fig. 3 show control *SR-BI*$^{+/-}$ and SR-BI KO eggs at metaphase II contained 40 sister chromatids (20 pairs) aligned on a spindle (Fig. 3, two leftmost columns, spindles perpendicular to the plane of the image). The other SR-BI KO eggs were classified, based on their chromosomal and spindle morphologies, into five categories, for which in Fig. 3 schematic representations (top row) and representative images at several magnifications (rightmost five columns) are shown. In each case, progression beyond MII was evident from the segregation of sister chromatids (40 at MII), leaving 20 single chromatids

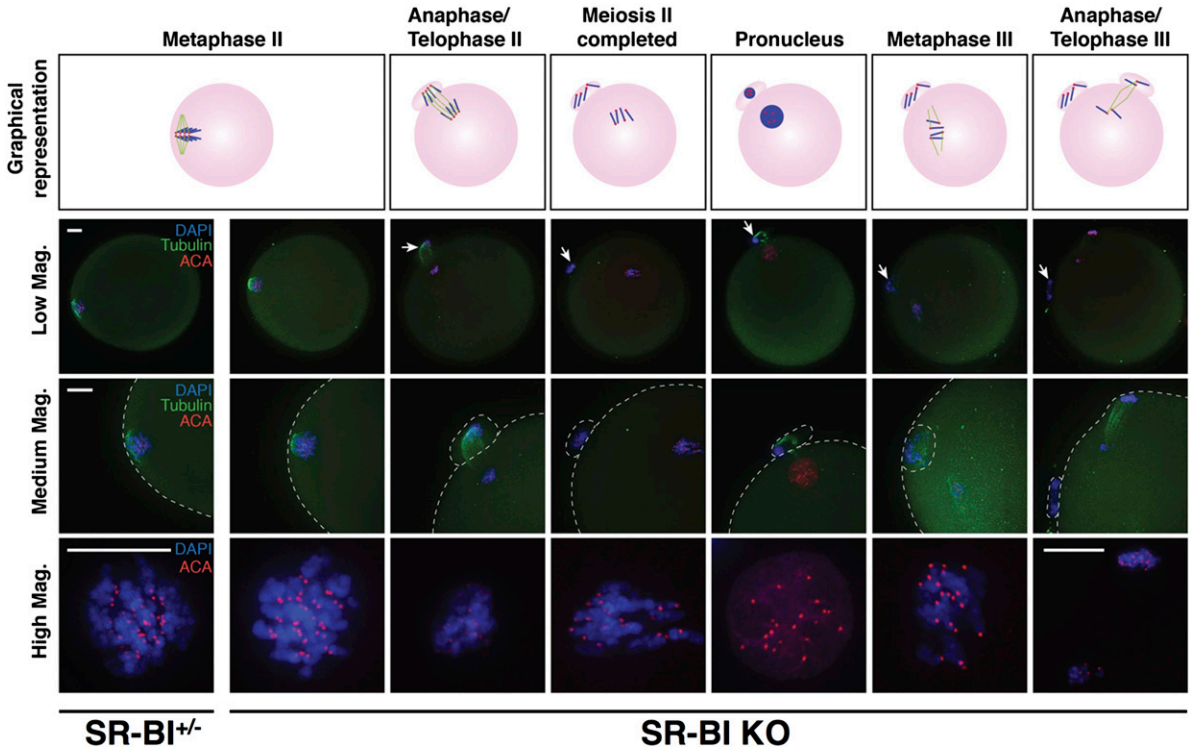

Fig. 3. Meiotic progression of oocytes from control *SR-BI*$^{+/-}$ and SR-BI KO mice assessed by deconvolution microscopy. *SR-BI*$^{+/-}$ and SR-BI KO females were superovulated, and oocytes were harvested ∼20 h after hCG administration and denuded by hyaluronidase treatment. The oocytes were stained to visualize chromosomes (DAPI; blue), microtubules (tubulin; green), centromeres [anticentromere antibody (ACA); red], and the nuclear membrane (lamin B1) (Fig. S1). Deconvolved and *z*-projected images were collected. Representative images of oocytes at various stages of meiosis (schematically indicated in the top row) are shown. For clarity, only 8 of 40 chromatids present at MII arrest are illustrated in the top row. Low magnification images (second row) show the overall morphology of the eggs; arrows indicate second polar bodies. Medium magnification images (third row) show the arrangement of the chromosomes and the spindle; dashed lines outline the cells and second polar bodies. High magnification images (bottom row) illustrate the numbers and arrangements of chromatids (red spots) in the eggs. High magnification images of the chromatids in representative polar bodies may be found in Fig. S2. Scale bars (10 μm) for each row are shown in the leftmost images, except that the magnification of the "high mag." image for anaphase/telophase III (lower rightmost panel) differs slightly from those of the other high magnification images as indicated by its own scale bar (10 μm).

within the egg and as expected, 20 single centromeres per second PB (Fig. 3 and Fig. S2). Formation of a pronucleus was confirmed by staining for lamin B1, a component of the nuclear lamina that would be indicative of exit from meiosis and entry into the first mitotic cell cycle (Fig. S1).

Most of the control *SR-BI*$^{+/-}$ eggs ($n = 8$) were either arrested at MII (Fig. 3, first column) or at an earlier stage at ∼16 (93% of eggs scored) or ∼20 h (89%) after hCG administration (induction of superovulation) (Table 1). In this experiment, a small fraction of the control *SR-BI*$^{+/-}$ eggs had progressed beyond MII. In addition, no WT *SR-BI*$^{+/+}$ eggs progressed beyond MII at ∼16 h ($n = 8$), indicating that the control *SR-BI*$^{+/-}$ eggs may exhibit a mild defect in MII arrest. In other experiments, we observed no differences in the very low level of spontaneous activation between WT and heterozygous mutant eggs. Table 1 shows a dramatic time-dependent increase in SR-BI KO eggs that had progressed past MII at ∼16 (73%) or ∼20 h (93%) (representative images are in Fig. 3).

Table 1. Quantitative morphologic analysis of spontaneous meiotic progression beyond MII arrest

	Hours after hCG administration			
	∼16		∼20	
Stage in meiotic progression	*SR-BI*$^{+/-}$ ($n = 30$)	SR-BI KO ($n = 11$)*	*SR-BI*$^{+/-}$ ($n = 9$)	SR-BI KO ($n = 27$)
At MII or earlier (%)	93	27	89	7
Beyond MII (%)	7	73	11	93

*Four SR-BI KO oocytes at ∼16 h and two SR-BI KO oocytes at ∼20 h could not be scored, because the chromatin was too diffuse to reliably count centromeres.

Activation of ovulated eggs by either fertilization or parthenogenetic agents suppresses the kinase activities of MPF and MAPK that are required to maintain MII arrest (16, 17, 23). We determined the MPF and MAPK activities of lysates from ovulated eggs that were harvested 18 h after hCG administration, incubated for 6 h in M16 medium, and then, collected in pools of four eggs each: *SR-BI*$^{+/+}$, five pools; *SR-BI*$^{+/-}$, seven pools; SR-BI$^{-/-}$ (KO), nine pools (additional details in *SI Materials and Methods*). Few of the eggs from the *SR-BI*$^{+/+}$ (5 of 39) and SR-BI$^{+/-}$ (1 of 31) mice exhibited second PBs, whereas eggs from the SR-BI KO either did (all eggs in six pools) or did not (no eggs in three pools) exhibit second PBs. Fig. S3 shows that there were substantially lower MPF and MAPK activities in SR-BI KO eggs that spontaneously escaped MII arrest (e.g., second PB extrusion) compared with those without second PBs from both the control and the SR-BI KO mice. Thus, at least some of the biochemical processes that normally accompany egg activation were spontaneously induced in the ovulated SR-BI KO eggs that were activated.

Because most SR-BI KO eggs failed to arrest at MII, which was indicated by progression to anaphase/telophase II, completed meiosis II, pronuclear stage, metaphase III, or anaphase/telophase III (Fig. 1), and exhibited reduced MPF and MAPK

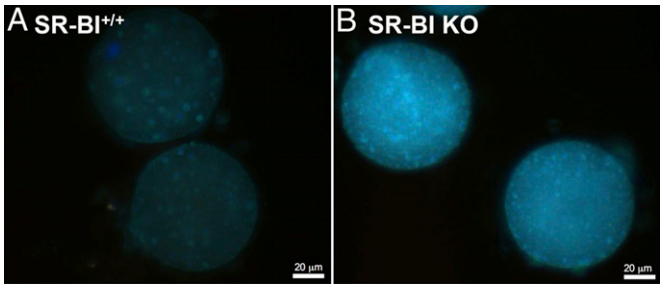

Fig. 4. Cholesterol levels in *SR-BI*$^{+/+}$ and SR-BI KO eggs. Eggs harvested ~16 h after hCG administration from superovulated (*A*) *SR-BI*$^{+/+}$ and (*B*) SR-BI KO mice on a mixed C57BL/6:129 background were denuded by hyaluronidase treatment, washed, incubated with 0.5 mg/mL Filipin III complex (Sigma), washed again, mounted on slides, and imaged by fluorescence microscopy (UV light excitation) as described in *SI Materials and Methods*. The images shown are representative of those observed in two independent experiments using at least six eggs for each genotype. (Scale bars: 20 μm.)

activities, impairment of cell cycle control may, in part, account for SR-BI KO female infertility, although other factors may contribute as well.

Abnormally High Cholesterol Deposition in SR-BI KO Eggs. In SR-BI KO mice, high cholesterol deposition in RBCs and platelets, caused at least in part by the high UC content of HDL, contributes to diverse abnormalities of these cells (5, 9, 10, 12, 13). We suspected that SR-BI KO eggs might have abnormally high cholesterol accumulation that might contribute to the spontaneous escape of ovulated SR-BI KO eggs from MII arrest. Thus, we measured the relative UC levels in ovulated eggs from hormone-primed mice by fluorescence microscopic analysis of cells stained with the cholesterol-binding fluorescent dye filipin (34). Fig. 4*A* shows that filipin fluorescence in control eggs from *SR-BI*$^{+/+}$ females exhibited a weak, uniform intensity together with somewhat brighter puncta. Similar results were observed using eggs from *SR-BI*$^{+/-}$ females. Eggs from SR-BI KO females (Fig. 4*B*) showed a similar staining pattern, except that the intensity of fluorescence was much stronger (68% ± 15% increase, $P = 0.004$) (Fig. S4). These results indicate the presence of abnormally high levels of UC in the SR-BI KO eggs and raise the possibility that excess UC in SR-BI KO eggs might be responsible for their abnormal escape from MII arrest and possibly might contribute to premature death. Loading cells with excess UC by various routes can induce endoplasmic reticulum (ER) stress, mitochondrial dysfunction, and mitochondrial-mediated cell death (35–41).

Effects of Excess Cholesterol Loading on WT Eggs. We directly assessed the ability to activate eggs from WT mice by loading them with excess cholesterol. Exogenous cholesterol was delivered by treating eggs for 10–45 min with 0.125 or 0.5 mM cholesterol-loaded MβCD (+ cholesterol) as indicated, a standard approach for increasing cellular cholesterol content (26, 42). For example, incubating *SR-BI*$^{+/+}$ eggs for 10 min at 37 °C with 0.5 mM cholesterol/MβCD increased relative UC by 38% ± 10% ($P = 0.019$) (Fig. S4). Eggs isolated from the oviducts of hormone-primed WT C57BL/6 females ~14–16 h after hCG administration were incubated with or without cholesterol/MβCD, washed to remove the cholesterol/MβCD, and then, incubated without cholesterol/MβCD for an additional 5–6 h at 37 °C. For comparison, some eggs were incubated for 6 h with the well-established chemical activator 5 mM $SrCl_2$ in calcium-free or 2 mM EGTA-containing medium.

We examined several phenotypes associated with egg activation, including (*i*) alterations in $[Ca^{2+}]_i$ measured immediately after cholesterol/MβCD addition (assessed using the Ca^{2+}-sensitive dye Fura-2AM), (*ii*) MPF and MAPK activities, (*iii*) second PB extrusion, (*iv*) stage in meiosis (deconvolution microscopy), and (*v*) subsequent cleavage to the two-cell stage. Fig. 5 shows typical time courses of the changes in the relative $[Ca^{2+}]_i$ after cholesterol addition for five individual WT C57BL/6 eggs continuously incubated with cholesterol/MβCD for 45 min. For all of the eggs that remained viable during the experiments ($n = 26$), the exposure to cholesterol/MβCD induced a single relatively steep increase in $[Ca^{2+}]_i$ after an ~15- to 34-min lag. For most of these eggs (24 of 26), the increase was transient, with a partial (3 of 24) or essentially complete (21 of 24) (Fig. 5) return to the baseline before the end of the 45-min imaging period. There was variation in the amplitude and width of the spikes in different eggs. The single spike in $[Ca^{2+}]_i$ was somewhat reminiscent of that seen when transient ethanol exposure induces activation (24, 25) and differed from the robust oscillations observed by $SrCl_2$ or fertilization-induced activation (18, 19, 21, 22, 43) (Fig. S5). We also performed $[Ca^{2+}]_i$ imaging experiments on eggs exposed to cholesterol/MβCD for 25 min, in which we imaged the eggs during cholesterol/MβCD exposure and then, after the cholesterol/MβCD was washed away. We observed a single large spike in $[Ca^{2+}]_i$ that returned to baseline when we collected data between 20 and 155 min after removing the cholesterol/MβCD (Fig. S6). There was no evidence of $[Ca^{2+}]_i$ oscillations induced by cholesterol/MβCD.

Fig. 6 shows that cholesterol loading for 20–25 min seemed to be as effective as $SrCl_2$ treatment in activating the eggs, which was assessed by suppression of MAPK and MPF kinase activities (Fig. 6*A*), induction of PB extrusion (Fig. 6 *B* and *C*), and progression to subsequent stages in meiosis (e.g., pronucleus formation) (Fig. 6*C*). All three assessments were made ~5–6 h after the addition of cholesterol or $SrCl_2$. Comparable cholesterol induction of second PB extrusion was observed using eggs from hormone-primed *SR-BI*$^{+/-}$ mice on a mixed C57BL/6:129 background (Fig. S7). We also measured second PB extrusion in WT C57BL/6 eggs during $[Ca^{2+}]_i$ imaging experiments, in which we imaged the eggs during the 25-min cholesterol/MβCD exposure and for an additional 155 min after the cholesterol/MβCD was washed away. A single $[Ca^{2+}]_i$ spike was observed in most of the

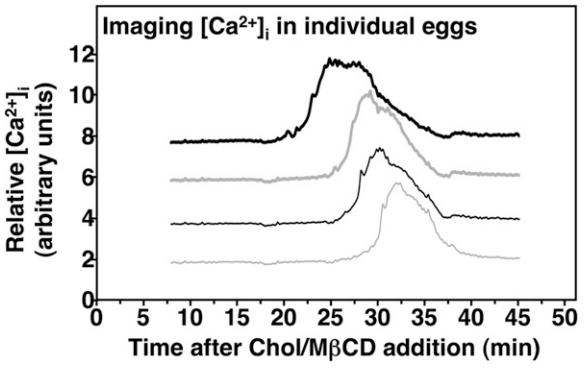

Fig. 5. Effects of cholesterol loading on $[Ca^{2+}]_i$ in eggs from WT C57BL/6 females. Eggs from WT C57BL/6 females were harvested ~14–16 h after hCG administration, stripped of cumulus cells using hyaluronidase, and loaded with the calcium-sensitive fluorescent dye Fura-2AM. The eggs were then placed at time = 0 in M2 medium supplemented with 0.125 mM cholesterol/MβCD (Chol/MβCD) at 37 °C. Relative $[Ca^{2+}]_i$ measured using an inverted microscope as a function of time (sampled every 10 s) was determined as the ratio of fluorescence intensities excited by 340- and 380-nm light. Eggs in Chol/MβCD-containing medium were continuously imaged, and the results for five typical eggs are shown displaced from each other on the *y* axis by 2 arbitrary units to prevent overlap. After 45 min of Chol/MβCD exposure, the eggs were washed and placed in Chol/MβCD-free M2 medium at 37 °C for an additional ~5.25 h, after which second PB extrusion was assessed.

viable eggs (16 of 18 in three independent experiments) (Fig. S6*B*), and 94% (15 of 16) of those eggs extruded a second PB by the end of the second 155-min cholesterol/MβCD-free incubation. Thus, multiple distinct $[Ca^{2+}]_i$ spikes were not required for cholesterol-induced second PB extrusion.

In multiple experiments, we found that most cholesterol/MβCD-activated eggs progressed to the two-cell stage 24 h after treatment. For example, in two such experiments, we followed for 24 h in vitro the fates of 0.125 ($n = 41$) or 0.5 mM ($n = 11$) cholesterol-loaded WT C57BL/6 eggs; of those eggs that extruded second PBs after 6 h (68% and 73%, respectively), 71% and 63%, respectively, underwent cleavage to the two-cell stage by 24 h after cholesterol loading. In contrast, untreated eggs remained arrested in MII. Strikingly, in our $[Ca^{2+}]_i$ imaging experiments on C57BL/6 eggs loaded with cholesterol for 25 min, of those eggs that were viable 24 h after treatment ($n = 29$), 90% extruded a second PB at ∼6 h ($n = 26$), 100% of which exhibited a Ca^{2+} spike. In addition, 86% of those activated eggs that were examined (19 of 22) were found to have progressed to the two-cell stage. Of the remaining three eggs that had not extruded a second PB, two eggs exhibited a Ca^{2+} spike, and none progressed to the two-cell stage (additional details in *SI Materials and Methods*). Thus, induction of a Ca^{2+} spike may be necessary but not sufficient for cholesterol/MβCD-induced egg activation. Future experiments will be required to determine which features of the Ca^{2+} spike (onset time, duration, amplitude, etc.) and the status of the eggs (e.g., extent of cholesterol loading) are necessary for activation. Taken together, our observations indicate that delivery of exogenous cholesterol to eggs efficiently induces exit from MII arrest by mechanisms that include biochemical changes associated with classic chemical-mediated activation and sperm-mediated activation during fertilization. Thus, cholesterol delivery can induce activation, suggesting that spontaneous activation caused by excess cholesterol in eggs of SR-BI KO females contributes directly to their female infertility.

Discussion

Female SR-BI KO mice exhibit fully penetrant infertility (6, 14). Our previous findings that these animals have essentially normal ovarian histology and that their fertility can be readily rescued by an HDL cholesterol-lowering drug suggested that the infertility might be a consequence of defects in oocytes or eggs, possibly caused by the animals' unusual dyslipidemia (hypercholesterolemia with abnormal HDL structure and composition) (2, 6, 7, 14, 15). Indeed, defects occurring during or soon after ovulation in vivo are readily apparent, because ∼19% of the eggs harvested ∼16 h after hCG administration (hormone-induced superovulation) are dead (refs. 6 and 14 and this study).

Here, we sought to understand the cellular basis of SR-BI KO female infertility by investigating oocyte growth and meiotic progression. We observed no obvious defects in oocyte growth in the follicle, maintenance of primary meiotic arrest in prophase I, resumption of meiosis after release from primary arrest (kinetics of GVBD), or efficiency of first PB extrusion (Fig. 1 shows a schematic depiction of meiosis and parthenogenesis). However, when we examined ovulated eggs from control and SR-BI KO females, we found that substantial numbers of SR-BI KO eggs had spontaneously activated (escaped MII arrest and exhibited second PB extrusion and suppression of MFP and MAPK activities). Deconvolution immunofluorescence imaging of the untreated, viable SR-BI KO eggs harvested at ∼16 or ∼20 h after hCG administration established that the progressive spontaneous escape from MII arrest resulted in second PB extrusion, pronucleus formation, and progression to metaphase III and

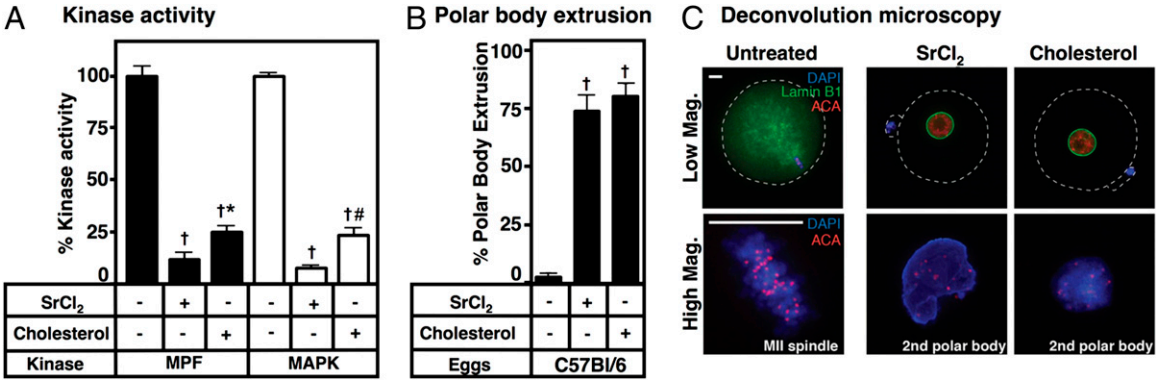

Fig. 6. Additional effects of cholesterol loading and $SrCl_2$ treatment on eggs from WT C57BL/6 females. (*A–C*) Eggs from WT C57BL/6 females were harvested ∼14–16 h after hCG administration and stripped of cumulus cells by hyaluronidase treatment. (*A*) MAPK and MPF kinase activities. Eggs were pretreated for 25 min without (–) or with (+) 0.125 mM cholesterol-loaded MβCD (Cholesterol) in M16 at 37 °C as indicated. They were then washed and incubated in M16 medium either without [for untreated ($n = 60$) or cholesterol-loaded MβCD ($n = 68$) eggs] or with 5 mM $SrCl_2$/2 mM EGTA ($n = 40$) at 37 °C for 6 h. Eggs were then washed, pooled into sets of four, and lysed, and MAPK and MPF kinase activities were measured as described in *SI Materials and Methods*. The values represent the averages ± SEMs from four independent assays using eggs harvested and processed on 7 different d. The values for one-way ANOVA for MPF and MAPK activities were $P < 0.00001$. *P value < 0.02 (unpaired Student t test) for comparisons with $SrCl_2$; †P value < 0.0001 (unpaired Student t test) for comparisons with untreated controls; #P value < 0.001(unpaired Student t test) for comparisons with $SrCl_2$. (*B*) PB extrusion. Some of the eggs ($n = 124$) were pretreated at 37 °C for 25 min with (+) 0.125 mM cholesterol-loaded MβCD (Cholesterol) in M16 medium and then washed and incubated in M16 medium for an additional 6 h at 37 °C. The remaining eggs were incubated for 6 h at 37 °C in M16 medium without ($n = 103$) or with ($n = 114$) 5 mM $SrCl_2$/2 mM EGTA. The fraction of eggs exhibiting second PB extrusion was then determined (averages from eight independent experiments). The value for one-way ANOVA was $P < 0.00001$. †P value < 0.0001 (paired Student t test) for comparisons with untreated controls. (*C*) Deconvolution microscopy. Eggs were pretreated for 20 min without (–) or with (+) 0.5 mM cholesterol-loaded MβCD (Cholesterol) in M16 at 37 °C as indicated. They were then washed and incubated in M16 medium either without [for untreated ($n = 20$) or cholesterol-loaded ($n = 20$) eggs] or with 5 mM $SrCl_2$/2 mM EGTA ($n = 17$) at 37 °C for 6 h. We then stained the cells and collected deconvolved and z-projected images as described in Fig. 3. (*Upper*) Low-magnification images show the overall morphology of the eggs; dashed lines outline the cells and the second PBs. (*Lower*) High-magnification images show the number and arrangement of chromatids in either the main cell [untreated; 40 paired centromeres (red) at the MII spindle] or the second PBs ($SrCl_2$ and cholesterol). The fractions of eggs that extruded a second PB were untreated, 0% (0 of 18); $SrCl_2$, 77% (10 of 13); and cholesterol/MβCD, 74% (14 of 19). Those eggs that were fragmented at the end of the 6-h incubation (untreated, two; $SrCl_2$, four; cholesterol, one) were not included in the calculation of the percentage exhibiting second PB exclusion. ACA, anticentromere antibody. (Scale bar: 10 μm.)

anaphase/telophase III. Spontaneous fertilization-independent exit from MII (or inability to establish or maintain arrest at MII) results in cells with a haploid chromosome complement, which in at least some cases, is further reduced during subsequent progression to metaphase III and anaphase/telophase III. These cellular defects are likely to account for at least some and perhaps most of the inability of ovulated SR-BI eggs to be fertilized and develop normally into viable embryos after mating (6). Additional studies are necessary to determine whether the SR-BI KO eggs that were dead at harvesting ~16 h posthormone induction died because of meiotic defects or if other independent abnormalities also contributed to this process.

Cholesterol Accumulation in SR-BI KO Eggs Contributes to Their Abnormal Phenotypes. One potential mechanism underlying premature death and spontaneous escape from MII arrest of SR-BI KO eggs is their abnormal accumulation of cholesterol. Indeed, excess cholesterol accumulation in RBCs and platelets in SR-BI KO mice, apparently caused by the high UC:TC ratio in circulating HDL (7, 8), has previously been associated with the abnormal maturation, lifetime, structure, and/or function of these blood cells (7, 9–13). As was the case for RBCs and platelets in SR-BI KO mice, we detected excess cholesterol in ovulated SR-BI KO eggs (here assessed by filipin staining). In complementary experiments, we found that cholesterol loading of control, fertile, *SR-BI*$^{+/-}$, or WT eggs by incubation with a cholesterol/MβCD complex resulted in activation similar to that of SR-BI KO eggs as well as a single spike in $[Ca^{2+}]_i$. Prolonged accumulation of excess cholesterol might also contribute through various routes (e.g., ER stress, mitochondrial dysfunction, and excessive or prolonged $[Ca^{2+}]_i$ elevation) to the premature death of some of the SR-BI KO eggs (35–41, 44, 45). We, therefore, conclude that (*i*) cholesterol can induce parthenogenetic activation of mouse eggs and that (*ii*) accumulation of excess cholesterol in SR-BI KO oocytes plays a substantial role in generating their abnormal phenotypes and consequently, the infertility of SR-BI KO females. Conversely, Buschiazzo et al. (46) have shown that cholesterol depletion by exposure to high levels of cholesterol-free MβCD (15 mM for 30 min at 37 °C) induces a delay in second PB extrusion and a low fertilization of mouse eggs. We have found that pretreating *SR-BI*$^{+/-}$ and SR-BI KO eggs with 10 mM cholesterol-free MβCD reduces filipin staining and is severely toxic (81% and 88% reduced viability, respectively). Taken together, these data suggest that cholesterol in mouse eggs must be maintained within a relatively narrow physiological range to ensure the oocyte's health and developmental potential. A critical role of UC in mediating oocyte/egg abnormalities is consistent with our previous report that correcting the abnormal composition (high UC:TC ratio) of plasma HDL can restore fertility (7, 10, 14). It is possible that excess cholesterol-independent mechanisms may also be involved.

HDL Is the Likely Source of Excess Cholesterol in SR-BI KO Eggs. Four lines of surgical transplantation, genetic, and pharmacologic evidence support the hypothesis that abnormal circulating HDL in SR-BI KO mice (high UC:TC ratio and large diameter) (5, 7, 8) is a major cause of female SR-BI KO infertility and likely to be the cause of excess cholesterol accumulation in their eggs. (*i*) Ovary transplantation established that ovarian expression of SR-BI is not necessary for fertility during embryonic development (primordial follicle production) or adult maturation and function (primordial follicle conversion to antral follicles and ovulation). SR-BI KO ovaries bilaterally transplanted into SR-BI–positive hosts developed the capacity to ovulate functional eggs that can be fertilized and generate healthy pups (14). (*ii*) Tissue-specific transgenic expression of SR-BI in the liver of SR-BI KO mice restores not only normal HDL composition and structure but also, essentially normal fertility (15). (*iii*) In SR-BI KO mice, homozygous genetic ablation of the gene encoding apoA-I, the major protein component of HDL, reduces total plasma cholesterol (mainly HDL cholesterol) to essentially WT levels, although the HDL particles remain abnormally large. Fertility is partially restored in these double KO mice (41% fertility and small litter sizes) (14). (*iv*) Oral administration of the HDL cholesterol-lowering drug probucol reduces total plasma cholesterol to WT levels and restores to essentially normal the UC content of HDL, although the HDL particles remain abnormally large (7, 14). Fertility of SR-BI KO females is restored soon after probucol treatment (14). Several studies indicate that the abnormal UC composition (high UC:TC ratio) rather than the increased size of HDL particles in SR-BI KO mice may play a particularly important role in SR-BI KO female infertility. As noted above, apoA-I deficiency and probucol treatment partially or nearly fully restore fertility to SR-BI KO mice without substantially reducing the abnormally large size of HDL particles. Also, transgenic expression of the human cholesterol ester transfer protein in SR-BI KO mice reduces the size/density of the HDL in a dose-dependent fashion (47, 48). Although the size of the HDL particles in these transgenic SR-BI KO mice is normalized, the composition is not (abnormally high UC:TC ratio), and they are infertile (48).

There are two attractive mechanisms by which abnormal HDL particles in the follicular fluid of antral follicles in SR-BI KO mice might lead to excess cholesterol accumulation in oocytes. Because of the relatively small size of HDL particles compared with other lipoproteins, HDL in many animals is the only lipoprotein present in substantial amounts in the follicular fluid that bathes the developing oocyte in the antral follicle (49–52). It may be that, in the follicle, the UC-enriched HDL particles transfer cholesterol to the oocytes directly, which they seem to do in RBCs and platelets (9, 10), or indirectly (e.g., through surrounding cumulus cells). Su et al. (53) have suggested that mouse preovulatory oocytes synthesize little cholesterol and obtain cholesterol primarily from the surrounding cumulus cells. Thus, there seems to be a mechanism that could transfer HDL-derived cholesterol from cumulus cells to the oocytes. An alternative mechanism for excess cholesterol accumulation in SR-BI KO oocytes is that normal cholesterol homeostasis in oocytes may depend on adequate levels of HDL-mediated cholesterol efflux to balance input and that the UC-enriched HDL particles in SR-BI KO mice may be unable to mediate sufficient cholesterol efflux to prevent excess cholesterol accumulation.

HDL has been shown to have multiple activities, including the ability to transport lipids other than cholesterol [e.g., vitamin E (54) and sphingosine-1-phosphate (55)] and influence oxidation, inflammation, metabolism, chemotaxis, thrombosis, microbial infection, cell signaling, and others (56–58). Thus, it is possible that, in addition to contributing to accumulation of excess cholesterol in oocytes, some of the effects of the abnormal HDL on female fertility in SR-BI KO mice may be independent of its role in cholesterol transport.

Excess Cholesterol and Egg Activation. One possible mechanism by which excess cholesterol might activate eggs is its stimulation of an increase in cytoplasmic $[Ca^{2+}]$, possibly by inducing ER Ca^{2+} release through a stress pathway or by otherwise influencing calcium channel or pump activities. Normally, fertilization or parthenogenetic agents (e.g., $SrCl_2$/EGTA or ethanol) induce a single spike or oscillations in $[Ca^{2+}]_i$ that are important for activation and successful progression of embryonic development (18, 19, 24, 25, 43).

Excess cholesterol-induced escape from MII arrest is unlikely to involve all of the same mechanisms as those induced by the MEK inhibitor U0126 (blocks MAPK activation) (23, 59, 60), c-mos deficiency (23, 61), or Zn depletion (25, 62, 63) because of their differing phenotypes. Both c-mos KO and Zn-insufficient eggs share with SR-BI eggs an otherwise spontaneous exit from MII arrest (64). However, unlike SR-BI KO eggs, c-mos KO and

Zn-insufficient eggs often extrude abnormally large first PBs (64). Aged eggs—those not fertilized within a critical time after ovulation (65–68)—also are subject to relatively high rates of spontaneous activation that involves exit from MII arrest, second PB extrusion, arrest at a metaphase III-like stage (abnormal spindle and no pronucleus), and cell death (fragmentation and apoptosis) (68, 69). Future studies will be required to characterize in detail the mechanisms underlying excess cholesterol-induced activation. Those future studies will help determine if cholesterol-induced activation might serve as an alternative to $SrCl_2$-induced or other (70) activation methods and perhaps, even improve efficiency in procedures, such as somatic cell nuclear transfer, to derive embryonic stem cells from nuclear transfer blastocysts or generate cloned animals (70, 71).

Implications for Human Infertility. This study has uncovered a previously unidentified ability of excess cholesterol to activate MII-arrested mouse eggs. In addition, this report raises the possibility that abnormalities in cholesterol metabolism in general and SR-BI–mediated cholesterol metabolism specifically (6, 7, 14) have the potential to contribute to human female infertility of unknown etiology (72, 73). In such cases, pharmacologic manipulation of cholesterol metabolism (e.g., lowering excess cholesterol in oocytes or eggs) might prove beneficial. It is noteworthy that Velasco et al. (74) and Yates et al. (75) have reported a potential influence of variations in SR-BI on fertility of women undergoing in vitro fertilization (IVF). In one study, Velasco et al. (74) found that SR-BI levels in granulosa cells from 50 volunteers were correlated with plasma levels of estradiol and the number of retrieved and fertilized oocytes, although SR-BI levels were not correlated with quality measurements of embryos, primary diagnosis of infertility, or pregnancy outcomes. A study of 274 women by Yates et al. (75) found no association of the SR-BI alleles tested with qualitative measures of embryo viability (blastocyst number and grade). However, 0 of 10 heterozygous carriers of one minor allele (rs4238001) had viable fetuses after embryo transfer, raising the possibility that this minor allele (and another allele in an African-American subset of subjects) may possibly contribute to human female infertility. A recent report suggests that there may be an association of high-plasma UC in males and females and increased time to pregnancy in 501 couples (76). In addition, the report of a case of human infertility caused by spontaneous activation (77) raises the possibility that excess cholesterol-induced egg activation may have clinical relevance.

Despite the progress in assisted reproduction in the last decades, infertility remains an unresolved medical problem. Recent data indicate that there are more than 30 million women with infertility of unknown origin (78). Additional studies will determine if and to what extent variations in SR-BI activity specifically or cholesterol deposition in oocytes or eggs generally might influence human female fertility.

Materials and Methods

Pure C57BL/6 (Charles River Laboratories, Jackson Laboratory, and Taconic), *SR-BI*$^{-/-}$, *SR-BI*$^{+/-}$, and *SR-BI*$^{+/+}$ (5) mice were maintained on an RMH3000 laboratory diet ad libitum, and experiments were performed in concordance with the guidelines from the committees for animal care at the Massachusetts Institute of Technology and Pontificia Universidad Católica de Chile (*SI Materials and Methods*). Oocytes were collected from unprimed or primed females, oocyte and follicle diameters were measured, in vitro maturation of oocytes was performed, eggs were activated with $SrCl_2$/EGTA, cholesterol was depleted by MβCD or delivered by cholesterol/ MβCD complexes, relative cholesterol content was assessed using filipin staining, eggs were imaged by whole-mount staining and deconvolution microscopy, and statistical analyses were performed using standard procedures (*SI Materials and Methods*).

ACKNOWLEDGMENTS. We thank Helen Skaletsky for helpful suggestions, Junmei Yao and Alan Discua for technical assistance, and Cindy Woolley for help in preparing the manuscript. This work was supported by National Institutes of Health (NIH) grants (to D.F.A. and M.K.), NIH Pre-Doctoral Training Grant T32GM007287 (to L.W.), an MIT International Science and Technology Initiatives Chile Cooperative Grant (to A.Y., D.B., A.R., and M.K.), Chilean National Council for Scientific and Technological Research Program Inserción en la Academia Grant 79090028 (to D.B.), Chilean National Council for Scientific and Technological Research Program Fondo Nacional de Desarrollo Científico y Tecnológico Grants 11090064 and 1141236 (to D.B.) and 1110712 (to A.R.), and the Howard Hughes Medical Institute (D.C.P.).

1. Acton S, et al. (1996) Identification of scavenger receptor SR-BI as a high density lipoprotein receptor. *Science* 271(5248):518–520.
2. Rigotti A, Miettinen HE, Krieger M (2003) The role of the high-density lipoprotein receptor SR-BI in the lipid metabolism of endocrine and other tissues. *Endocr Rev* 24(3):357–387.
3. Krieger M (2001) Scavenger receptor class B type I is a multiligand HDL receptor that influences diverse physiologic systems. *J Clin Invest* 108(6):793–797.
4. Saddar S, Mineo C, Shaul PW (2010) Signaling by the high-affinity HDL receptor scavenger receptor B type I. *Arterioscler Thromb Vasc Biol* 30(2):144–150.
5. Rigotti A, et al. (1997) A targeted mutation in the murine gene encoding the high density lipoprotein (HDL) receptor scavenger receptor class B type I reveals its key role in HDL metabolism. *Proc Natl Acad Sci USA* 94(23):12610–12615.
6. Trigatti B, et al. (1999) Influence of the high density lipoprotein receptor SR-BI on reproductive and cardiovascular pathophysiology. *Proc Natl Acad Sci USA* 96(16): 9322–9327.
7. Braun A, et al. (2003) Probucol prevents early coronary heart disease and death in the high-density lipoprotein receptor SR-BI/apolipoprotein E double knockout mouse. *Proc Natl Acad Sci USA* 100(12):7283–7288.
8. Out R, et al. (2004) Scavenger receptor class B type I is solely responsible for the selective uptake of cholesteryl esters from HDL by the liver and the adrenals in mice. *J Lipid Res* 45(11):2088–2095.
9. Dole VS, et al. (2008) Thrombocytopenia and platelet abnormalities in high-density lipoprotein receptor-deficient mice. *Arterioscler Thromb Vasc Biol* 28(6):1111–1116.
10. Holm TM, et al. (2002) Failure of red blood cell maturation in mice with defects in the high-density lipoprotein receptor SR-BI. *Blood* 99(5):1817–1824.
11. Meurs I, et al. (2005) HDL cholesterol levels are an important factor for determining the lifespan of erythrocytes. *Exp Hematol* 33(11):1309–1319.
12. Brodde MF, et al. (2011) Native high-density lipoproteins inhibit platelet activation via scavenger receptor BI: Role of negatively charged phospholipids. *Atherosclerosis* 215(2):374–382.
13. Korporaal SJ, et al. (2011) Deletion of the high-density lipoprotein receptor scavenger receptor BI in mice modulates thrombosis susceptibility and indirectly affects platelet function by elevation of plasma free cholesterol. *Arterioscler Thromb Vasc Biol* 31(1): 34–42.
14. Miettinen HE, Rayburn H, Krieger M (2001) Abnormal lipoprotein metabolism and reversible female infertility in HDL receptor (SR-BI)-deficient mice. *J Clin Invest* 108(11):1717–1722.
15. Yesilaltay A, et al. (2006) Effects of hepatic expression of the high-density lipoprotein receptor SR-BI on lipoprotein metabolism and female fertility. *Endocrinology* 147(4): 1577–1588.
16. Marston AL, Amon A (2004) Meiosis: Cell-cycle controls shuffle and deal. *Nat Rev Mol Cell Biol* 5(12):983–997.
17. Von Stetina JR, Orr-Weaver TL (2011) Developmental control of oocyte maturation and egg activation in metazoan models. *Cold Spring Harb Perspect Biol* 3(10):a005553.
18. Schultz RM, Kopf GS (1995) Molecular basis of mammalian egg activation. *Curr Top Dev Biol* 30:21–62.
19. Sobinoff AP, Sutherland JM, Mclaughlin EA (2013) Intracellular signalling during female gametogenesis. *Mol Hum Reprod* 19(5):265–278.
20. Fraser LR (1987) Strontium supports capacitation and the acrosome reaction in mouse sperm and rapidly activates mouse eggs. *Gamete Res* 18(4):363–374.
21. Kline D, Kline JT (1992) Repetitive calcium transients and the role of calcium in exocytosis and cell cycle activation in the mouse egg. *Dev Biol* 149(1):80–89.
22. Liu L, Trimarchi JR, Keefe DL (2002) Haploidy but not parthenogenetic activation leads to increased incidence of apoptosis in mouse embryos. *Biol Reprod* 66(1):204–210.
23. Phillips KP, et al. (2002) Inhibition of MEK or cdc2 kinase parthenogenetically activates mouse eggs and yields the same phenotypes as Mos(-/-) parthenogenotes. *Dev Biol* 247(1):210–223.
24. Cuthbertson KSR, Whittingham DG, Cobbold PH (1981) Free Ca2+ increases in exponential phases during mouse oocyte activation. *Nature* 294(5843):754–757.
25. Rogers NT, et al. (2006) The absence of a Ca(2+) signal during mouse egg activation can affect parthenogenetic preimplantation development, gene expression patterns, and blastocyst quality. *Reproduction* 132(1):45–57.
26. Zidovetzki R, Levitan I (2007) Use of cyclodextrins to manipulate plasma membrane cholesterol content: Evidence, misconceptions and control strategies. *Biochim Biophys Acta* 1768(6):1311–1324.
27. Carabatsos MJ, Sellitto C, Goodenough DA, Albertini DF (2000) Oocyte-granulosa cell heterologous gap junctions are required for the coordination of nuclear and cytoplasmic meiotic competence. *Dev Biol* 226(2):167–179.

28. Carabatsos MJ, Elvin J, Matzuk MM, Albertini DF (1998) Characterization of oocyte and follicle development in growth differentiation factor-9-deficient mice. *Dev Biol* 204(2):373–384.
29. Li R, Albertini DF (2013) The road to maturation: Somatic cell interaction and self-organization of the mammalian oocyte. *Nat Rev Mol Cell Biol* 14(3):141–152.
30. Kishigami S, Wakayama T (2007) Efficient strontium-induced activation of mouse oocytes in standard culture media by chelating calcium. *J Reprod Dev* 53(6):1207–1215.
31. Wang L, et al. (2008) Brefeldin A disrupts asymmetric spindle positioning in mouse oocytes. *Dev Biol* 313(1):155–166.
32. Markoulaki S, Matson S, Abbott AL, Ducibella T (2003) Oscillatory CaMKII activity in mouse egg activation. *Dev Biol* 258(2):464–474.
33. Cuthbertson KSR (1983) Parthenogenetic activation of mouse oocytes in vitro with ethanol and benzyl alcohol. *J Exp Zool* 226(2):311–314.
34. Norman AW, Demel RA, de Kruyff B, van Deenen LL (1972) Studies on the biological properties of polyene antibiotics. Evidence for the direct interaction of filipin with cholesterol. *J Biol Chem* 247(6):1918–1929.
35. Yao PM, Tabas I (2001) Free cholesterol loading of macrophages is associated with widespread mitochondrial dysfunction and activation of the mitochondrial apoptosis pathway. *J Biol Chem* 276(45):42468–42476.
36. Feng B, et al. (2003) The endoplasmic reticulum is the site of cholesterol-induced cytotoxicity in macrophages. *Nat Cell Biol* 5(9):781–792.
37. Tabas I (2010) The role of endoplasmic reticulum stress in the progression of atherosclerosis. *Circ Res* 107(7):839–850.
38. Kedi X, Ming Y, Yongping W, Yi Y, Xiaoxiang Z (2009) Free cholesterol overloading induced smooth muscle cells death and activated both ER- and mitochondrial-dependent death pathway. *Atherosclerosis* 207(1):123–130.
39. Malhotra JD, Kaufman RJ (2011) ER stress and its functional link to mitochondria: Role in cell survival and death. *Cold Spring Harb Perspect Biol* 3(9):a004424.
40. Montero J, et al. (2010) Cholesterol and peroxidized cardiolipin in mitochondrial membrane properties, permeabilization and cell death. *Biochim Biophys Acta* 1797(6-7): 1217–1224.
41. Bosch M, Marí M, Gross SP, Fernández-Checa JC, Pol A (2011) Mitochondrial cholesterol: A connection between caveolin, metabolism, and disease. *Traffic* 12(11):1483–1489.
42. Brown AJ, Sun L, Feramisco JD, Brown MS, Goldstein JL (2002) Cholesterol addition to ER membranes alters conformation of SCAP, the SREBP escort protein that regulates cholesterol metabolism. *Mol Cell* 10(2):237–245.
43. Wakai T, Fissore RA (2013) Ca(2+) homeostasis and regulation of ER Ca(2+) in mammalian oocytes/eggs. *Cell Calcium* 53(1):63–67.
44. Gordo AC, et al. (2002) Intracellular calcium oscillations signal apoptosis rather than activation in in vitro aged mouse eggs. *Biol Reprod* 66(6):1828–1837.
45. Ozil JP, et al. (2005) Egg activation events are regulated by the duration of a sustained [Ca2+]cyt signal in the mouse. *Dev Biol* 282(1):39–54.
46. Buschiazzo J, et al. (2013) Cholesterol depletion disorganizes oocyte membrane rafts altering mouse fertilization. *PLoS ONE* 8(4):e62919.
47. Harder C, Lau P, Meng A, Whitman SC, McPherson R (2007) Cholesteryl ester transfer protein (CETP) expression protects against diet induced atherosclerosis in SR-BI deficient mice. *Arterioscler Thromb Vasc Biol* 27(4):858–864.
48. Hildebrand RB, et al. (2010) Restoration of high-density lipoprotein levels by cholesteryl ester transfer protein expression in scavenger receptor class B type I (SR-BI) knockout mice does not normalize pathologies associated with SR-BI deficiency. *Arterioscler Thromb Vasc Biol* 30(7):1439–1445.
49. Shalgi R, Kraicer P, Rimon A, Pinto M, Soferman N (1973) Proteins of human follicular fluid: The blood-follicle barrier. *Fertil Steril* 24(6):429–434.
50. Perret B-P, et al. (1985) Lipoprotein and phospholipid distribution in human follicular fluids. *Fertil Steril* 43(3):405–409.
51. Le Goff D (1994) Follicular fluid lipoproteins in the mare: Evaluation of HDL transfer from plasma to follicular fluid. *Biochim Biophys Acta* 1210(2):226–232.
52. Jaspard B, et al. (1996) Biochemical characterization of pre-beta 1 high-density lipoprotein from human ovarian follicular fluid: Evidence for the presence of a lipid core. *Biochemistry* 35(5):1352–1357.
53. Su YQ, et al. (2008) Oocyte regulation of metabolic cooperativity between mouse cumulus cells and oocytes: BMP15 and GDF9 control cholesterol biosynthesis in cumulus cells. *Development* 135(1):111–121.
54. Mardones P, et al. (2002) Alpha-tocopherol metabolism is abnormal in scavenger receptor class B type I (SR-BI)-deficient mice. *J Nutr* 132(3):443–449.
55. Karuna R, et al. (2011) Plasma levels of sphingosine-1-phosphate and apolipoprotein M in patients with monogenic disorders of HDL metabolism. *Atherosclerosis* 219(2): 855–863.
56. Mineo C, Shaul PW (2012) Novel biological functions of high-density lipoprotein cholesterol. *Circ Res* 111(8):1079–1090.
57. Soran H, Hama S, Yadav R, Durrington PN (2012) HDL functionality. *Curr Opin Lipidol* 23(4):353–366.
58. Zhu X, Parks JS (2012) New roles of HDL in inflammation and hematopoiesis. *Annu Rev Nutr* 32:161–182.
59. Lee B, et al. (2006) Phosphorylation of IP3R1 and the regulation of [Ca2+]i responses at fertilization: A role for the MAP kinase pathway. *Development* 133(21):4355–4365.
60. Matson S, Ducibella T (2007) The MEK inhibitor, U0126, alters fertilization-induced [Ca2+]i oscillation parameters and secretion: Differential effects associated with in vivo and in vitro meiotic maturation. *Dev Biol* 306(2):538–548.
61. Araki K, et al. (1996) Meiotic abnormalities of c-mos knockout mouse oocytes: Activation after first meiosis or entrance into third meiotic metaphase. *Biol Reprod* 55(6): 1315–1324.
62. Moses RM, Kline D (1995) Release of mouse eggs from metaphase arrest by protein synthesis inhibition in the absence of a calcium signal or microtubule assembly. *Mol Reprod Dev* 41(2):264–273.
63. Suzuki T, Yoshida N, Suzuki E, Okuda E, Perry ACF (2010b) Full-term mouse development by abolishing Zn2+-dependent metaphase II arrest without Ca2+ release. *Development* 137(16):2659–2669.
64. Bernhardt ML, Kim AM, O'Halloran TV, Woodruff TK (2011) Zinc requirement during meiosis I-meiosis II transition in mouse oocytes is independent of the MOS-MAPK pathway. *Biol Reprod* 84(3):526–536.
65. Kubiak JZ (1989) Mouse oocytes gradually develop the capacity for activation during the metaphase II arrest. *Dev Biol* 136(2):537–545.
66. Zhang N, Wakai T, Fissore RA (2011) Caffeine alleviates the deterioration of Ca(2+) release mechanisms and fragmentation of in vitro-aged mouse eggs. *Mol Reprod Dev* 78(9):684–701.
67. Miao YL, Kikuchi K, Sun QY, Schatten H (2009) Oocyte aging: Cellular and molecular changes, developmental potential and reversal possibility. *Hum Reprod Update* 15(5): 573–585.
68. Chebotareva T, Taylor J, Mullins JJ, Wilmut I (2011) Rat eggs cannot wait: Spontaneous exit from meiotic metaphase-II arrest. *Mol Reprod Dev* 78(10-11):795–807.
69. Fissore RA, Kurokawa M, Knott J, Zhang M, Smyth J (2002) Mechanisms underlying oocyte activation and postovulatory ageing. *Reproduction* 124(6):745–754.
70. Tachibana M, et al. (2013) Human embryonic stem cells derived by somatic cell nuclear transfer. *Cell* 153(6):1228–1238.
71. Markoulaki S, Meissner A, Jaenisch R (2008) Somatic cell nuclear transfer and derivation of embryonic stem cells in the mouse. *Methods* 45(2):101–114.
72. Smith S, Pfeifer SM, Collins JA (2003) Diagnosis and management of female infertility. *JAMA* 290(13):1767–1770.
73. Chandra A, Martinez GM, Mosher WD, Abma JC, Jones J (2005) Fertility, family planning, and reproductive health of U.S. women: Data from the 2002 National Survey of Family Growth. *Vital Health Stat 23* 25(2005):1–160.
74. Velasco M, et al. (2006) Association of lower plasma estradiol levels and low expression of scavenger receptor class B, type I in infertile women. *Fertil Steril* 85(5): 1391–1397.
75. Yates M, Kolmakova A, Zhao Y, Rodriguez A (2011) Clinical impact of scavenger receptor class B type I gene polymorphisms on human female fertility. *Hum Reprod* 26(7):1910–1916.
76. Schisterman EF, et al. (2014) Lipid concentrations and couple fecundity: The LIFE study. *J Clin Endocrinol Metab* 99(8):2786–2794.
77. Combelles CM, Kearns WG, Fox JH, Racowsky C (2011) Cellular and genetic analysis of oocytes and embryos in a human case of spontaneous oocyte activation. *Hum Reprod* 26(3):545–552.
78. van der Poel SZ (2012) Historical walk: The HRP Special Programme and infertility. *Gynecol Obstet Invest* 74(3):218–227.